2021 IEEE/RSJ International Conference on Intelligent Robots and Systems (IROS)
September 27 - October 1, 2021. Prague, Czech Republic

2021 IEEE/RSJ International Conference on Intelligent Robots and Systems (IROS) | 978-1-6654-1714-3/21/$31.00 ©2021 IEEE | DOI: 10.1109/IROS51168.2021.9636420

Origami Logic Gates for Printable Robots

Wenzhong Yan[1,†], Chang Liu[2], and Ankur Mehta[2]

Abstract— **Origami robots–often called "printable" robots–created using folding processes have gained extensive attention due to their potential for rapid and accessible design and fabrication through simple structures with complex functionalities. However, almost all origami robots require conventional rigid electronics for control, which may hinder the integration and restrict the potential of these origami systems. Here we introduce origami logic gates that can be built through folding. The major enabling technology is a bistable switch that can switch between two different circuits to control the electrical flow. Based on the origami switch, we develop NOT, AND, and OR logic gates (showing functional completeness) and demonstrate these logic gates through sufficiently powering low-current LEDs. These logic gates are fabricated using cut-and-fold manufacturing and offer a potential way of integrating logic functions directly into origami machines without electronics.**

I. INTRODUCTION

Cut-and-fold printable robots are created through a design and fabrication strategy inspired by the ancient art of origami and from nature [1]. Starting with a single 2D sheet of paper or even a 1D linear string, complex 3D objects with distinct properties can be constructed by folding [2]. This origami-inspired strategy enables constructing a wide range of robotic morphologies and functionalities [3]–[6]. Such origami-inspired devices have several potential advantages, including rapid design and fabrication [7], low cost and high accessibility [8], high strength-to-weight ratio [9], [10], built-in compliance for safe interaction with humans [11], compact storage and transport [12], reconfigurability [13] and self-folding [14], [15], and high scalablility to be still practical at micro/nano-scale [16]. However, almost all origami robots rely on discrete or otherwise external electronics for control, which restricts the potential of origami robots. Therefore, an origami-inspired non-electronic solution for control would open new avenues for autonomous origami robots.

Recently, there are attempts among scientists and engineers to explore the feasibility of harnessing origami/kirigami for computation to eliminate electronics. Meng et al. proposed mechanical logic gates based on a bistability-based foldable waterbomb origami consisting of bistable kirigami units [17]. They demonstrated AND, OR, and NOT gates that enable mechanical computing which takes pure mechanical signals, i.e. deformation/force, as inputs/outputs. These mechanical logic gates function through interaction between structural components; yet, they still need electronics to actuate the mechanical signals, which may hamper their practical applications. On the basis of an origami waterbomb and active materials, origami mechanologic has been developed enabling seamless integration of sensing, computation, and reflexes into the compliant bodies of robotics [18]. However, this mechanologic is passively controlled by environmental factor, i.e. humidity, which greatly limits the operation speed and application scenario. Novelino et al. explored a magneto-mechano-electrical origami Kresling pattern for digital computing through a distributed magnetic actuation, allowing for on-the-fly programmability and computation [19]. This mechanism, nevertheless, requires a bulky and complicated magnetic actuation setup for remote control, leading to increased system complexity.

Here, we report origami logic gates (including NOT, AND, and OR gates) that can be fabricated by the cut-and-fold method without external electronics. Our design is based on an origami switch that harnesses the snap-through instability of a flexible bistable beam to switch between two different circuits, thus controlling the flow of electrical currents. The output electrical energy can be directly used to drive end effectors or other downstream mechanisms. The snap-through instability endows the switch and its associated logic gate with key functional properties: (i) The state of the switch is binary ("open" or "closed"), which allows high signal-to-noise ratio (SNR) control outputs, despite uncertainties (e.g. noise or non-linearity) associated with the applied actuation mechanisms [20] or electrical inputs. (ii) The switch requires power only when it switches between the two states; otherwise it passively remains in its most recently driven state [21]. The states of the switch is controlled by a pair of CSCP actuators [22]; the switch changes its states when the corresponding actuator drives the bistable beam reaching its switching point. The CSCP actuator acts as a thermal actuator and can be driven through Joule heating (similar to shape memory alloy (SMA) actuators).

Based on the bistable switch, we design origami logic gates of NOT, AND, and OR with functional completeness by configuring the electrical connectivity of the switch terminals. Although the output resistance is relatively high, the logic gates can be potentially directly used to control end effectors, which we currently demonstrate through sufficiently powering a light-emitting diode (LED), which only requires very low supply current. These switches and logic gates are fabricated using origami-inspired cut-and-fold manufacturing (with electrical power being the only off-board, non-printable element of the complete system), offering a rapid design and fabrication strategy for building robots. This work offers a way of embodying logic functions directly into origami

[1]Wenzhong Yan is with Department of Mechanical and Aerospace Engineering, University of California, Los Angeles, CA 90095, USA. [2]Chang Liu and Ankur Mehta are with the Department of Electrical and Computer Engineering, University of California, Los Angeles, CA 90095, USA.
[†] Corresponding author, wzyan24@g.ucla.edu

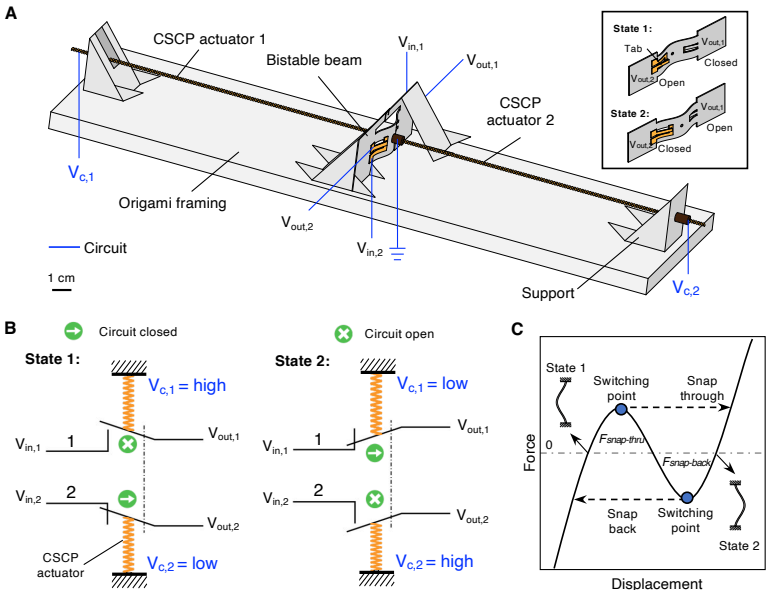

Fig. 1. An origami bistable switch mainly composed of a bistable beam and two CSCP actuators. (A) 3D structure of the switch. Insert: two states of the bistable beam. (B) The schematic of the bistable switch with labels. (C) A bifurcation diagram of the bistable beam.

mechanisms, leading towards autonomous control of fully printable origami robots without rigid or bulky electronic components.

The remainder of the paper is organized as follows: in Section II, we introduce the mechanism, design, and fabrication of the origami switch; in Section III, we present the origami NOT, AND, and OR logic gates; and the conclusion is presented in Section IV.

II. The Origami Bistable Switch

A. Mechanism

The basic design of the origami bistable switch is shown in Fig. 1A. It mainly consists of a bistable beam and two CSCP actuators. One end of each actuator is attached on the bistable beam while the other is fixed on an origami framing. Thus, the actuators can drive the bistable beam switch between two stable states to control the on/off states of two electrical circuits on the beam (see the insert of Fig. 1A). When the beam is actuated by actuator 1, it stays at state 1 with the pole 1 closed and pole 2 open, and vise versa. The mechanism of the bistable switch is described in Fig. 1B. The bistable beam is represented by a modified double-pole-single-throw switch where two poles are always at opposite states.

The snap-through instability of the bistable beam is the key enabling technology, allowing binary and minimal-energy operation of the switch. The instability of the beam can be described by using a bifurcation diagram, one axis being the force that actuation mechanism generate and the other one being the displacement of the beam (Fig. 1C) [23]. Initially, we assume the beam stays at state 1. As the applied force increases (i.e., as the actuator 1 is powered), the beam bends rightwards and finally reaches the switching point (i.e. $F_{\text{snap-thru}}$). Consequently, the beam snaps through and rests at state 2. Due to the energy storage during bending driven by the actuator, the beam can release it energy in a rapid "snapping" motion, jumping to the other stable state (i.e. state 2). When a opposite force is applied, the beam again has to overcome energy barrier to return to state 1. To overcome this energy barrier, another actuator (i.e. actuator 2) is used.

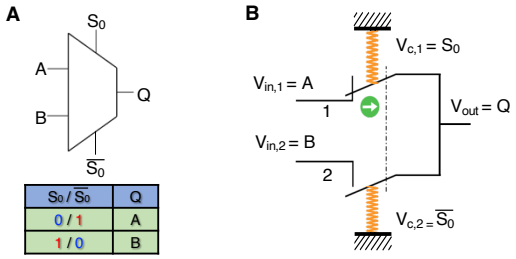

Fig. 2. An origami bistable switch with its two outputs connected together, functioning as a nonvolatile multiplexer. (A) Logic diagram and true table of a 2-to-1 nonvolatile multiplexer having two inputs A and B, one output Q, and one selection S_0 (with its complementary $\overline{S_0}$) terminals. (B) The schematic of an origami 2-to-1 nonvolatile multiplexer reconfigured from the bistable switch.

When the terminals of loop 1 and 2 are connected to a common output Q, the switch functions similarly as a non-volatile 2-to-1 multiplexer that selects between two analog or digital input signals (A and B) and forwards the selected input based on a select signal, S_0 (with its complementary $\overline{S_0}$, see Fig. 2). The switch chooses signal A when the select signal S_0 = 0 and the signal B, when the select signal $\overline{S_0}$ = 1. The logic function of the switch is:

$$Q = \overline{S_0} \cdot A + S_0 \cdot B \tag{1}$$

B. Design

To enable the functionality of the bistable switch, we need to guarantee that the CSCP actuators are powerful enough

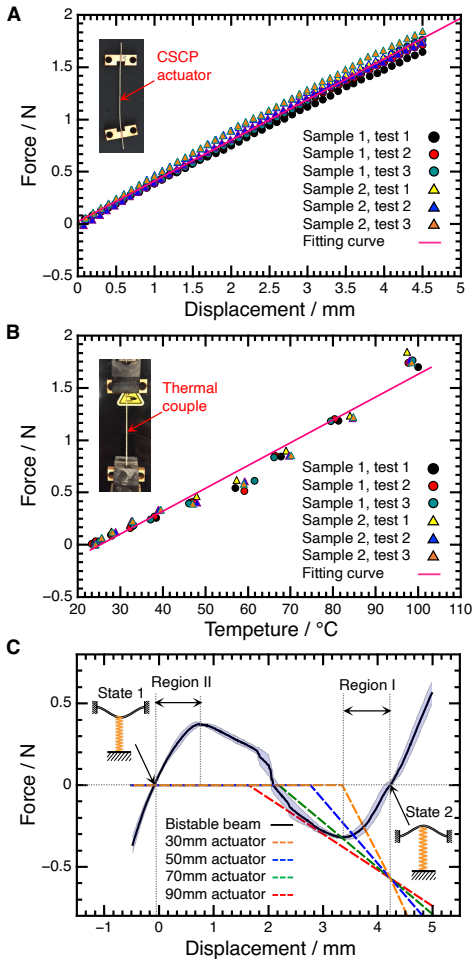

Fig. 3. Design of the origami bistable switch. (A) The force-displacement curve of 50-mm actuators in room temperature. (B) The exerted force of the actuators as a function of its temperature when heated up through Joule heating. A thermal couple was attached on the actuator as the insert shows. (C) The force-displacement curves of the chosen bistable beam and actuators with various length. Activation is guaranteed when the contraction force generated by the actuator is greater than the beam's activation force in region I. In region II, the bistable beam can snap back if there is another actuator pulling on it in the opposite direction (not shown in the graph).

to drive the bistable beam reaching its switching point; the mechanism of CSCP actuators in isolation has been well investigated and modeled in [22]. We observed the same response in our experiments so that we can directly apply the knowledge into our study. The thermo-electric-mechanical model of the actuator is as follows [22]:

$$F_{\mathrm{a}} = k(x_{\mathrm{a}} - x_0) + b_{\mathrm{a}}\dot{x_{\mathrm{a}}} + c_{\mathrm{T}}(T - T_0) \qquad (2)$$

where F_{a}, x_{a} and x_0 are the generated force, the loaded and unloaded length of the actuator, and k, b_{a} are the mean stiffness and mean damping of the actuator, respectively. k is inversely proportional to the length of the CSCP actuator. T is the temperature of the actuator, and T_0 is the room temperature (i.e. 23.9°C). c_{T} is a constant representing the mean slope that compensates the temperature rise. Due to the low speed operation, we ignore the term $b_{\mathrm{a}}\dot{x}$, as the effect of damping is considered negligible. In our experiment, we

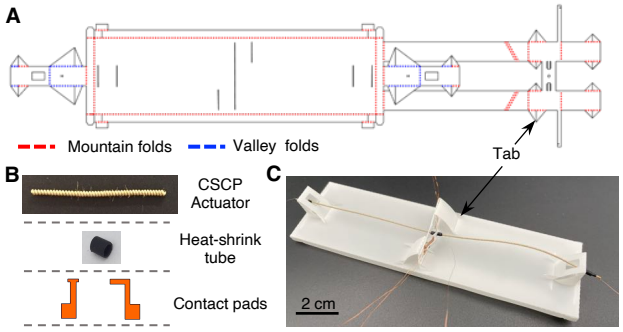

Fig. 4. Fabrication of the origami bistable switch. (A) 2D pattern of the origami frame. Red dashed lines represent mountain folds and blue lines are valley folds. (B) A list of essential components for the assembly. (C) Assembled origami switch.

characterized 50.0 mm actuators and obtained that k = -0.39 N/mm, and c_T = 2.18 × 10^{-2} N/°C by the methods in [22] (Fig. 3A and B).

The bistable beam used in this paper is created out of a polyester (PET) sheet and characterized by its displacement-force relationship as shown in black in Fig. 3C, featuring a switching force measured to be about 0.35 N. In this work, we assume that the maximum working temperature of the actuator is 50 °C (lower than the glass transition temperature of the bistable beam) to ensure the durability of the switch. By changing the length of the actuator, we can tune the attenuation of the output force against its contraction. As shown in the graph, the contraction force of a longer actuator tends to decrease much more slowly. With this theory, we are able to choose the actuator of 70 mm that can generate enough force to activate the selected bistable beam; the force generated by this CSCP actuator is always greater than the activation force of the bistable beam, guaranteeing a snap-through motion, in Region I. Through experiment measurement, we found the the critical control voltage of the actuator is about 3.6 V with a moderate cooling air to protect the switch from accident overheating and decided to use 4.2 V for all experiment to guarantee the actuation.

C. *Fabrication*

The fabrication of the switch consists of two consecutive steps: (i) origami cut-and-fold and (ii) assembly with actuator and contact pads. We built the origami frame of the switch by patterning a flexible, polyester film (DuraLar™, Grafix Plastics) with a cutting machine (Silhouette CAMEO 2, Silhouette America, Inc.). The 2D fabrication pattern of the switch is shown in Fig. 4A, where red dashed lines mean mountain folds and blue dashed lines represent valley folds. The connections between origami structures were reinforced by origami tabs minimizing resources required to assemble the devices. The bistable beam was precisely formed through a out-off-plane folding. More details about the fabrication of origami framing can be found in [24].

Then we assembled the electrical design of the switch in two main steps: (i) The two patterned contact pads (copper

tapes), i.e. a T-shaped pad and a L-shaped pad, were aligned and attached bistable beam to form the contact circuitry as shown in Fig. 3B. (ii) One terminal of each CSCP actuator (detailed fabrication can be found in [8]) was fixed to the beam by using a piece of heat-shrink tubing (7496K81, Insultab) on either side. The other terminals were similarly fixed to support structures (Fig. 3C).

D. Characterization

Figure 5A shows an origami bistable switch (with its two output connected together) that acts as a multiplexer between two different sources of electrical power. The loop 1 is grounded (0V), and the loop 2 is connected to a constant voltage, $V_{in,2}$. When the beam is at state 1, the pole 2 is open while the pole 1 remains closed, and the output of the switch is 0V. When a control voltage $V_{c,1}$ (= 4.2 V) is applied to the actuator 1, the beam snaps upward, opening the pole 1 while closing pole 2 with its output connected to the constant voltage, $V_{in,2}$. When a second control voltage, $V_{c,1}$ (= 4.2 V), is applied to the actuator 2, the beam snaps back and switches the output back to the 0 V.

Since the input circuit and control circuit are independent, the switch can be used for signal amplification. Figure 5B shows the response of the switch to 10-s-long voltage pulses of $V_{c,1}$ = 4.2 V as the input signal and supply voltage up to 11 V, which corresponds to a gain (voltage amplification) of 2.6. The gate delay is about 5 s in our experiment. This delay in switching results is mainly determined by the time needed for the actuator to heat up sufficiently to initiate the bistable beam's snap-through. This gate delay can be dramatically reduced by increasing control voltage, elongating the actuator, or reducing the critical switching force of the bistable beam. The detailed characterizations of this thermal delay is beyond the scope of this paper, and can be found in [25].

The hysteresis of the beam makes the operation of the switch robust to noise and enables the use of the switch as a signal noise filter. Noise in the control signal will not transmits to the output when it is moderate compared to the critical control voltage (i.e. 3.7V). To demonstrate this property, we applied two types of voltage pulses of $V_{c,1}$ = 4.2V to the actuator 1. Both types of voltage pulse are superposed with noise signal as shown in red in Fig. 5C. The noise is superposed on the first type of voltage pulse on its valley while is on the mountain of the second one. Because the amplitude of the noise was smaller than the critical switching voltage of the switch, it did not affected the output voltage (i.e., the switch effectively filtered the noise, Fig. 5C).

III. Origami Logic Gates

Based on the bistable switch, we can conduct all fundamental binary operators, such as NOT, AND and OR. To establish a context with which to understand digital logic, we assigned voltage V = 0V the binary value "0" and voltage V = 4.2 V (or 2.4 V, this is special for powering LED) the binary value "1".

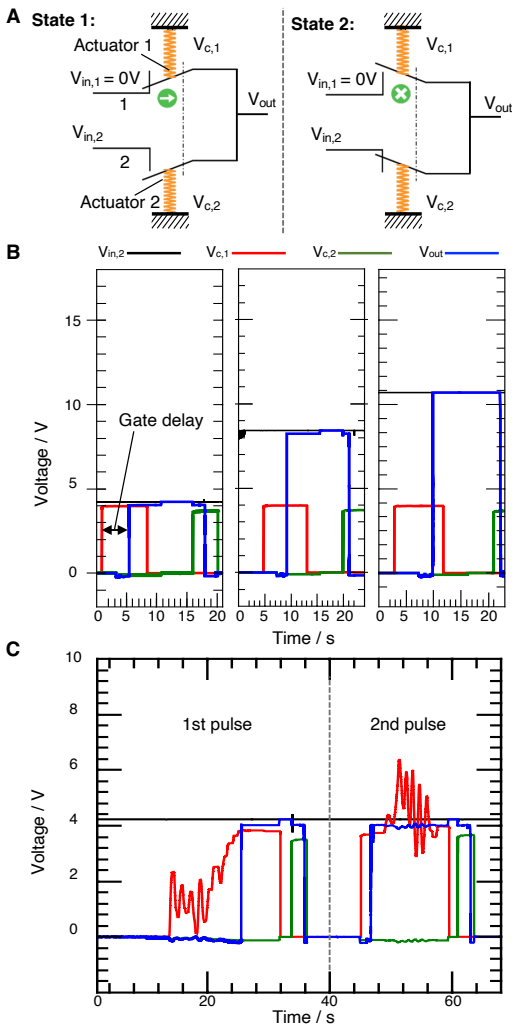

Fig. 5. Characterization of a bistable switch. (A) Two states of the reconfigurable switch with labels (B) Output of the switch for different $v_{in,2}$ values with control input ($v_{c,1}$ = 4.2 V) with an average gate delay, about 5 s. (C) Response of the switch to two rectangular pulses ($v_{c,1}$ = 4.2 V) as the control input. Random noise is superposed to both pulses at different phases.

A. NOT gate

A NOT gate inverts its input signal; an input of 0 generates an output of 1, and vice versa. The truth table for a NOT gate illustrates this behavior by summarizing the inputs and corresponding outputs (Fig. 6A). We built a origami NOT logic gate by setting $V_{in,1}$ = 2.4 V (binary 1) and $V_{in,2}$ and $V_{c,2}$ = 0 V (binary 0) by connecting these inputs to sources of constant voltage; in this configuration, output Q (i.e. V_{out}) varied only with $V_{c,1}$ which is assigned as the input A (Fig. 6B). When A = 0, the actuator is at rest remaining the bistable beam at its original state; the output of the system is connected to $V_{in,1}$, i.e. Q = 1, which is indicated by a green LED (Fig. 6C, left picture). When the input is changed to 1, the corresponding actuator drives the switch snap through; the output of the system becomes 0 since the pole 1 is open while pole 2 closed (see Supplementary Video S1 for the full demonstration). The result is presented as in Fig. 6C, right

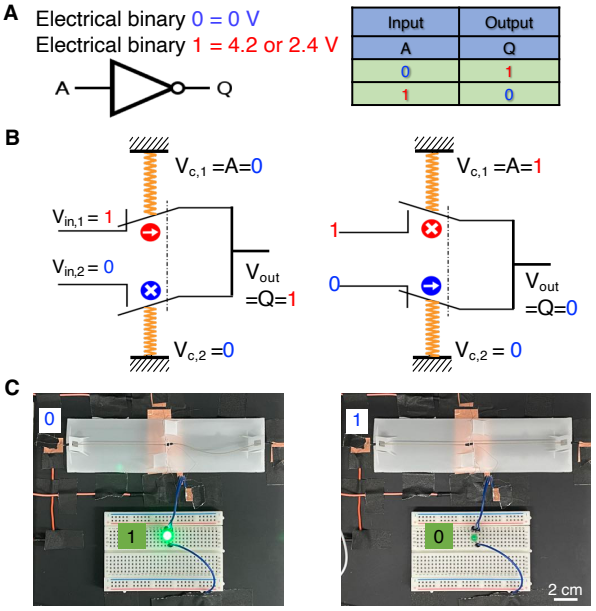

Fig. 6. An origami NOT gate. (A) Logic diagram and true table of a NOT gate. (B) The schematic of an origami NOT gate in our architecture. (C) The experimental demonstration of the NOT gate with a green LED as the indicator.

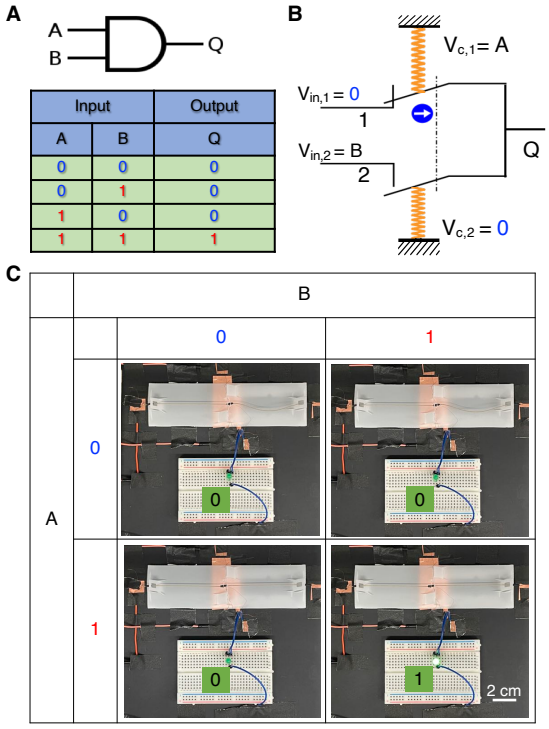

Fig. 7. An origami AND gate. (A) Logic diagram and true table of an AND gate. (B) The schematic of an origami AND gate. (C) The experimental demonstration of the AND gate with a green LED as the indicator.

picture. Since it is an nonvolatile NOT gate, it can store the memory until being reset by applying a high voltage to $V_{in,2}$ to activate the actuator 2 to drive the bistable beam back to state 1.

B. AND gate

The same bistable switch can be reprogrammed as both AND and OR logic gates by modifying the input voltage connections. AND and OR gates each require two inputs, in contrast with the NOT gate, which required only one input. An AND gate has two binary inputs, A and B. The output Q of an AND gate is 1 only when inputs A and B are both 1; otherwise, it is 0 (Fig. 7A). The switch is configured as an AND gate by assigning $V_{c,1}$ = A, $V_{in,2}$ = B, and $V_{in,1}$ and $V_{in,2}$ are connected to a constant source of voltage of value 0 (= 0 V) (Fig. 7B). In this configuration, when input B = 0, output Q is always 0 independent of the value of input A. Only when input A = 1 (thus making the beam to snap through), switching the output to connect with loop 2, and input B = 1 leads the output of the logic gate to become Q = 1. We demonstrated the logic operation of the AND gate experimentally with all four possible inputs (Fig. 7C).

C. OR gate

An OR gate, on the other hand, can output 1 when at least one of two inputs is 1; otherwise, it is 0 (Fig. 8A). This functionality can be realized by rearranging the inputs and connections of a origami bistable switch (Fig. 8B). The $V_{in,2}$ is reconfigured as high voltage, 1, with $V_{c,1}$ = A and $V_{in,1}$ = B. $V_{c,2}$ is used as a reset to erase the memory of last operation. In this configuration, it is only possible for the OR gate to output 0 when both A and B = 0. Otherwise, the output either is connected to $V_{in,2}$ = 1 or $V_{in,1}$ = B = 1. We experimentally demonstrated the functionality of the OR gate in all possible input configurations by using a green LED as the indicator (Fig. 8C).

IV. CONCLUSIONS

Origami machines have various attractive features, including rapid design and fabrication, low cost, light weight, and safe collaboration with humans [2]. Despite these remarkable advantages, the autonomy of origami machines is still challenging; control usually requires rigid electronics and associated bulky transmissions and transducers. This dependency impedes the integration and limits the capabilities of resulting origami machines. This work proposes basic origami logic gates (i.e., NOT, AND, and OR) for the control of origami robots without electronics. They theoretically could be employed as basic elements and further integrated into other logic gates and more complicated combinational circuits. These demonstrate a step towards autonomous origami robots and smart printable mechanisms purely through cut-and-fold without electronics. However, these logic gates currently have relatively high output resistance, which limits their capability of driving typical electrical-mediated actuators, e.g., shape memory alloy actuators (often requiring currents from hundreds of mA to more than an ampere) to achieve meaningful applications for integrated autonomous robots.

Currently, the success rate of the switches and logic gates are relatively low due to the non-optimized design of the tabs on the bistable beams, which usually leads to short

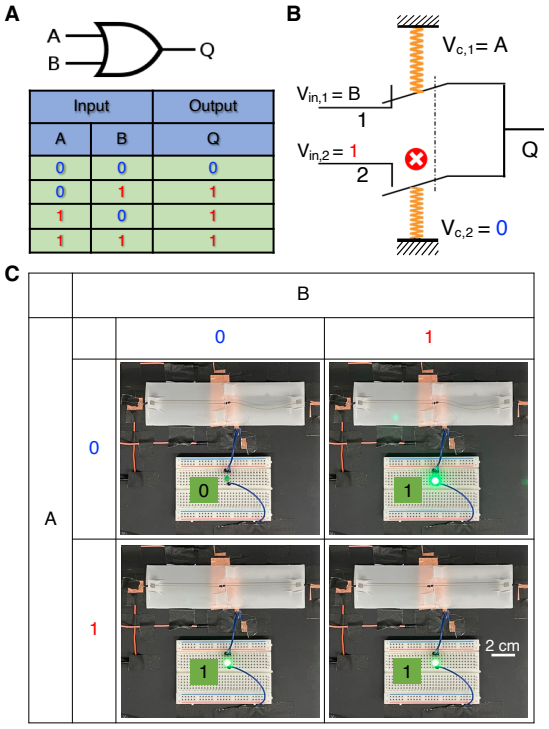

Fig. 8. An origami OR gate. (A) Logic diagram and true table of an OR gate. (B) The schematic of an origami OR gate in our architecture. (C) The experimental demonstration of the OR gate with a green LED as the indicator.

circuit where two tabs are forced to close simultaneously during snap-through. This factor greatly hinders the proposed mechanisms to meaningful applications for printable robots. For further study, we plan to explore the optimization of the design of the bistable switches.

The switches and logic gates are built of non-rigid sheet materials and conductive threads through origami-inspired folding. This approach allows integrated and monolithic design and rapid fabrication, leads to accessible, low cost, and potentially disposable designs [2], making it an attractive alternative to non-origami rigid systems that require electronic controls components. The resulting integrated systems are lightweight, low-cost, compliant, electronic-free, and nonmagnetic, enabling practical applications in extreme environments e.g. with high magnetic field or high radiation.

ACKNOWLEDGMENT

This work is partially supported by the National Science Foundation under grant #1752575.

REFERENCES

[1] K. Saito, S. Nomura, S. Yamamoto, R. Niiyama, and Y. Okabe, "Investigation of hindwing folding in ladybird beetles by artificial elytron transplantation and microcomputed tomography," *Proceedings of the National Academy of Sciences*, vol. 114, no. 22, pp. 5624–5628, 2017.

[2] D. Rus and M. T. Tolley, "Design, fabrication and control of origami robots," *Nature Reviews Materials*, vol. 3, no. 6, pp. 101–112, 2018.

[3] A. Pagano, T. Yan, B. Chien, A. Wissa, and S. Tawfick, "A crawling robot driven by multi-stable origami," *Smart Materials and Structures*, vol. 26, no. 9, p. 094007, 2017.

[4] D.-Y. Lee, S.-R. Kim, J.-S. Kim, J.-J. Park, and K.-J. Cho, "Origami wheel transformer: A variable-diameter wheel drive robot using an origami structure," *Soft robotics*, vol. 4, no. 2, pp. 163–180, 2017.

[5] Y. Chen, H. Wang, E. F. Helbling, N. T. Jafferis, R. Zufferey, A. Ong, K. Ma, N. Gravish, P. Chirarattananon, M. Kovac, *et al.*, "A biologically inspired, flapping-wing, hybrid aerial-aquatic microrobot," *Science Robotics*, vol. 2, no. 11, 2017.

[6] J. Cui, T.-Y. Huang, Z. Luo, P. Testa, H. Gu, X.-Z. Chen, B. J. Nelson, and L. J. Heyderman, "Nanomagnetic encoding of shape-morphing micromachines," *Nature*, vol. 575, no. 7781, pp. 164–168, 2019.

[7] Z. Zhakypov, K. Mori, K. Hosoda, and J. Paik, "Designing minimal and scalable insect-inspired multi-locomotion millirobots," *Nature*, vol. 571, no. 7765, pp. 381–386, 2019.

[8] W. Yan, A. L. Gao, Y. Yu, and A. Mehta, "Towards autonomous printable robotics: Design and prototyping of the mechanical logic," in *International Symposium on Experimental Robotics*. Springer, 2018, pp. 631–644.

[9] S.-J. Kim, D.-Y. Lee, G.-P. Jung, and K.-J. Cho, "An origami-inspired, self-locking robotic arm that can be folded flat," *Science Robotics*, vol. 3, no. 16, 2018.

[10] C. Liu, W. Yan, and A. Mehta, "Computational design and fabrication of corrugated mechanisms from behavioral specifications," *arXiv preprint arXiv:2011.05298*, 2020.

[11] Y. Lin, G. Yang, Y. Liang, C. Zhang, W. Wang, D. Qian, H. Yang, and J. Zou, "Controllable stiffness origami "skeletons" for lightweight and multifunctional artificial muscles," *Advanced Functional Materials*, vol. 30, no. 31, p. 2000349, 2020.

[12] E. Hawkes, B. An, N. M. Benbernou, H. Tanaka, S. Kim, E. D. Demaine, D. Rus, and R. J. Wood, "Programmable matter by folding," *Proceedings of the National Academy of Sciences*, vol. 107, no. 28, pp. 12 441–12 445, 2010.

[13] J. T. Overvelde, J. C. Weaver, C. Hoberman, and K. Bertoldi, "Rational design of reconfigurable prismatic architected materials," *Nature*, vol. 541, no. 7637, pp. 347–352, 2017.

[14] S. Felton, M. Tolley, E. Demaine, D. Rus, and R. Wood, "A method for building self-folding machines," *Science*, vol. 345, no. 6197, pp. 644–646, 2014.

[15] C. Liu, A. Orlofsky, C. D. Kitcher, and S. M. Felton, "A self-folding pneumatic piston for mechanically robust origami robots," *IEEE Robotics and Automation Letters*, vol. 4, no. 2, pp. 1372–1378, 2019.

[16] P. W. Rothemund, "Folding dna to create nanoscale shapes and patterns," *Nature*, vol. 440, no. 7082, pp. 297–302, 2006.

[17] Z. Meng, W. Chen, T. Mei, Y. Lai, Y. Li, and C. Chen, "Bistability-based foldable origami mechanical logic gates," *Extreme Mechanics Letters*, vol. 43, p. 101180, Feb. 2021.

[18] B. Treml, A. Gillman, P. Buskohl, and R. Vaia, "Origami mechanologic," *Proceedings of the National Academy of Sciences*, vol. 115, no. 27, pp. 6916–6921, July 2018.

[19] L. S. Novelino, Q. Ze, S. Wu, G. H. Paulino, and R. Zhao, "Untethered control of functional origami microrobots with distributed actuation," *Proceedings of the National Academy of Sciences*, Sept. 2020.

[20] P. Rothemund, A. Ainla, L. Belding, D. J. Preston, S. Kurihara, Z. Suo, and G. M. Whitesides, "A soft, bistable valve for autonomous control of soft actuators," *Science Robotics*, vol. 3, no. 16, 2018.

[21] Y. Song, R. M. Panas, S. Chizari, L. A. Shaw, J. A. Jackson, J. B. Hopkins, and A. J. Pascall, "Additively manufacturable micro-mechanical logic gates," *Nature communications*, vol. 10, no. 1, pp. 1–6, 2019.

[22] M. C. Yip and G. Niemeyer, "On the control and properties of supercoiled polymer artificial muscles," *IEEE Transactions on Robotics*, vol. 33, no. 3, pp. 689–699, June 2017.

[23] W. Yan, Y. Yu, and A. Mehta, "Analytical modeling for rapid design of bistable buckled beams," *Theoretical and Applied Mechanics Letters*, vol. 9, no. 4, pp. 264–272, 2019.

[24] W. Yan and A. Mehta, "Towards one-dollar robots: An integrated design and fabrication strategy for electromechanical systems," *Robotica*, 2020.

[25] W. Yan, Y. Yu, and A. Mehta, "Rapid design of mechanical logic based on quasi-static electromechanical modeling," in *2019 IEEE/RSJ International Conference on Intelligent Robots and Systems (IROS)*. IEEE, 2019, pp. 5820–5825.